Molecular events in matrix protein metabolism in the aging kidney

Kavithalakshmi Sataranatarajan,[1,2] Denis Feliers,[1] Meenalakshmi M. Mariappan,[1,3] Hak Joo Lee,[1,3] Myung Ja Lee,[1] Robert T. Day,[1] Hima Bindu Yalamanchili,[1] Goutam G. Choudhury,[1,3,4] Jeffrey L. Barnes,[1,3] Holly Van Remmen,[1,2,4] Arlan Richardson[1,2,4] and Balakuntalam S. Kasinath[1,2,3]

[1]Department of Medicine, University of Texas Health Science Center, San Antonio, TX, 78229, USA
[2]The Barshop Institute for Longevity and Aging Studies, University of Texas Health Science Center, San Antonio, TX, 78229, USA
[3]South Texas Veterans Health Care System, San Antonio, TX, 78284, USA
[4]Geriatric Research, Education and Clinical Center, San Antonio, TX, 78284, USA

Summary

We explored molecular events associated with aging-induced matrix changes in the kidney. C57BL6 mice were studied in youth, middle age, and old age. Albuminuria and serum cystatin C level (an index of glomerular filtration) increased with aging. Renal hypertrophy was evident in middle-aged and old mice and was associated with glomerulomegaly and increase in mesangial fraction occupied by extracellular matrix. Content of collagen types I and III and fibronectin was increased with aging; increment in their mRNA varied with the phase of aging. The content of ZEB1 and ZEB2, collagen type I transcription inhibitors, and their binding to the collagen type Iα2 promoter by ChIP assay also showed age-phase-specific changes. Lack of increase in mRNA and data from polysome assay suggested decreased degradation as a potential mechanism for kidney collagen type I accumulation in the middle-aged mice. These changes occurred with increment in TGFβ mRNA and protein and activation of its SMAD3 pathway; SMAD3 binding to the collagen type Iα2 promoter was also increased. TGFβ-regulated microRNAs (miRs) exhibited selective regulation. The renal cortical content of miR-21 and miR-200c, but not miR-192, miR-200a, or miR-200b, was increased with aging. Increased miR-21 and miR-200c contents were associated with reduced expression of their targets, Sprouty-1 and ZEB2, respectively. These data show that aging is associated with complex molecular events in the kidney that are already evident in the middle age and progress to old age. Age-phase-specific regulation of matrix protein synthesis occurs and involves matrix protein–specific transcriptional and post-transcriptional mechanisms.
Key words: albuminuria; collagen; fibrosis; microRNAs; SMAD3; TGF beta.

Correspondence
Balakuntalam S. Kasinath, Department of Medicine, MC7882, University of Texas Health Science Center, 7703 Floyd Curl Drive, San Antonio TX 78229-3900, USA. Tel.: 210 567 4707; fax: 210 567 4712; e-mail: kasinath@uthscsa.edu

Introduction

It is well documented in humans that aging is associated with progressive replacement of functioning kidney parenchyma with extracellular matrix proteins (fibrosis), albuminuria, and reduction in renal clearance function. Global glomerulosclerosis increases with age, and the remaining functioning glomeruli undergo hypertrophy (Glassock & Rule, 2012). Mesangium expands (Zheng *et al.*, 2003), and the tubulointerstitium shows increased deposition of matrix proteins, focal fibrosis, tubular dilatation (Abrass *et al.*, 1995), and macrophage infiltration (Zheng *et al.*, 2004). The glomerular filtration rate (GFR) decreases in the elderly although it may be normal in up to a third of the elderly subjects (Lindeman *et al.*, 1985). Abnormal increase in urine albumin excretion is reported in the elderly population in the absence of hypertension, diabetes, or metabolic syndrome, and in association with normal GFR (Reed & Kopyt, 2011). Albuminuria is also increased in the aging rodents (Abrass *et al.*, 1995).

The mechanisms underlying these structural and functional changes are not well understood although several pathways have been suggested including a role for growth factors such as TGFβ (Choudhury & Levi, 2011). TGFβ is well known to promote accumulation of renal extracellular matrix proteins in the kidney in disparate conditions including diabetes and ureteral obstruction by both promoting their synthesis and inhibiting their degradation (Ka *et al.*, 2012; Samarakoon *et al.*, 2012). In addition to transcription, mRNA translation is a crucial step in the synthesis of proteins, and recent findings have assigned an important role for microRNAs (miRs) in the regulation of translation (Kasinath *et al.*, 2009). These noncoding, approximately 22 nucleotide-long RNAs inhibit mRNA translation by binding to the complementary 3′-untranslated region of target mRNA and promote its degradation; they may also affect other steps in the initiation and elongation phases of mRNA translation (Kasinath & Feliers, 2011). miRs have been shown to play an important role in renal physiology. Podocyte-specific deletion of Dicer, an endoribonuclease essential for miR production, results in glomerular and tubular lesions with massive proteinuria and accelerated death by 4 weeks of age (Ho *et al.*, 2008). TGFβ/Smad3 axis regulates the expression of miRs by promoting their maturation (Davis *et al.*, 2008). TGFβ augments the expression of miR-192 in conditions associated with renal fibrosis, for example, diabetes and obstructive nephropathy (Kato *et al.*, 2007; Chung *et al.*, 2010). miR-21 mediates pro-fibrotic effects of TGFβ/Smad3 axis in ureteral obstruction–associated renal fibrosis (Zhong *et al.*, 2011). However, the status of miRs in renal senescence has not been explored. In this study, we explored molecular pathways that participate in the accumulation of renal matrix proteins in a mouse model of aging with focus on TGFβ and miRs under its control.

Results

Clinical parameters

Random blood glucose concentrations were normal in all age groups (Table 1). Body weight was significantly increased in the middle-aged mice (18 months old) compared to young mice (4–6 months of age) with no significant change from middle age to old age (26–32 months of

Table 1 Data on blood glucose concentration, body weight, kidney weight, kidney to body weight ratio for young, middle-aged and old mice are shown

	Young	Middle-aged	Old
Blood sugar (mg dL^{-1})	112 ± 4.7	104 ± 5.6	101 ± 10
Body weight (g)	21.8 ± 0.5	26.2 ± 0.8***	24.5 ± 0.9*
Kidney weight (mg)	185 ± 23.8	277 ± 31.6*	350 ± 39**
Kidney/Body weight (mg g^{-1})	5.9 ± 0.2	7.1 ± 0.1**	8.8 ± 0.5***,†††

*$P < 0.05$, **$P < 0.01$, ***$P < 0.001$ vs. young, †††$P < 0.001$ vs. middle-aged mice by ANOVA (n = 6–10 mice in each group).

age). The kidney weight significantly increased in both middle-aged and old mice ($P < 0.05$ and $P < 0.01$ vs. young mice, respectively). When compared to young mice, the kidney weight corrected to body weight was significantly increased by 20% in the middle-aged mice ($P < 0.01$) and by 49% in old mice ($P < 0.001$) demonstrating kidney hypertrophy. The urinary albumin/creatinine ratio was significantly increased by about two- and threefold in the middle-aged and old mice, respectively ($P < 0.01$), with marked heterogeneity (Fig. 1A). Serum cystatin C level bears an inverse relationship with GFR and is employed as an index of renal clearance function in aging studies in mice (Kume *et al.*, 2010); it is reported to be more sensitive than serum creatinine in mouse models of kidney injury (Song *et al.*, 2009). There was a progressive increase in serum cystatin C level through the aging process, reaching significance in old age ($P < 0.05$ vs. young) with significant heterogeneity (Fig. 1B). These data are in agreement with aging-related renal functional deterioration in mice (Kume *et al.*, 2010); some mice may retain clearance function despite aging as shown in human subjects in the Baltimore Longitudinal Study on Aging (Lindeman *et al.*, 1985).

Changes in extracellular matrix

Computer-aided morphometric analysis showed an increase in the glomerular area by 37% in the middle-aged mice ($P < 0.01$) and 63% in the old mice ($P < 0.001$) compared to young mice; the difference in glomerular area between the middle-aged and old mice was also significant ($P < 0.05$; Fig. 2A,B). These data suggest that glomerular hypertrophy occurs with aging as a part of kidney hypertrophy (Table 1). The contribution of extracellular matrix to the glomerular enlargement
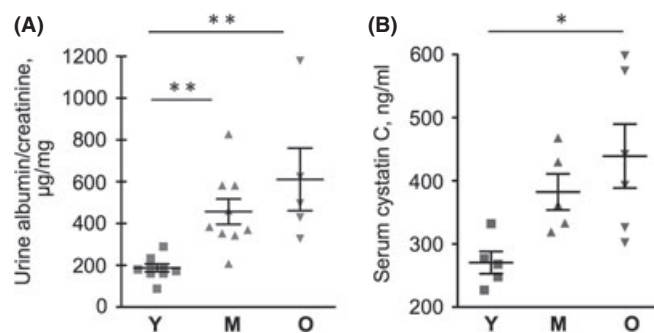

Fig. 1 Albuminuria and serum cystatin C levels in young (Y), middle-aged (M), and old (O) mice. (A) Urinary albumin to creatinine ratio in young (Y), middle-aged (M), and old (O) mice. Data from 5 to 9 mice in each group are shown (**$P < 0.01$ vs. young mice by ANOVA). (B) Serum cystatin C level bears an inverse relation to glomerular filtration function. Data from 5 to 6 mice in each group are shown (*$P < 0.05$ vs. young by ANOVA).
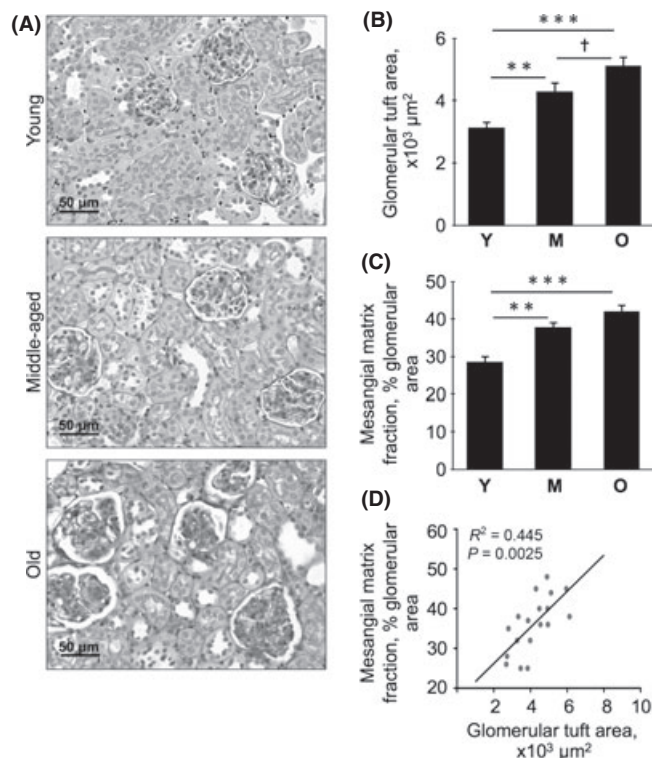

Fig. 2 Glomerular area and mesangial matrix fraction in young (Y), middle-aged (M), and old (O) mice. Kidney sections were stained with PAS (A), and glomerular area (B) and mesangial matrix fraction of the glomerulus (C) were measured by computer-aided morphometry. Representative micrographs from six mice in each of the three age groups are shown. Composite mean ± SE data from six mice in each group are shown in a histogram (**$P < 0.01$, ***$P < 0.001$ vs. young mice; †$P < 0.05$ vs. middle-aged mice by ANOVA). (D) Correlation between glomerular tuft area and mesangial matrix fraction of the glomerulus.

was assessed. PAS staining showed a progressive increase in PAS-positive mesangial area of the glomerulus by 33% in the middle-aged mice ($P < 0.01$) and by 40% in the old mice ($P < 0.001$; Fig. 2A,C). The percentage mesangial area occupied by PAS-positive material correlated directly with glomerular area ($r^2 = 0.445$, $P = 0.0025$; Fig. 2D). Because matrix proteins stain positive with the PAS stain, these data suggest that increase in extracellular matrix, that is, glomerulosclerosis, contributes importantly to the glomerular hypertrophy in the aging kidney.

To evaluate the status of extracellular matrix in the tubulointerstitium, we performed Sirius Red staining and examined it under polarized light, which detects types I and III collagen (Grimm *et al.*, 2003). Morphometry showed that there was an approximately fivefold ($P < 0.05$) and tenfold ($P < 0.001$) increase in the fractional area of staining in the tubulointerstitium in the middle-aged and old mice, respectively; the increment was also significant between the middle-aged mice and old mice ($P < 0.01$; Fig. 3A). Sirius Red staining was confirmed by immunoblotting for collagen types I and III. Thus, the content of collagen type Iα2 chain in the renal cortex increased by twofold in middle age ($P < 0.001$) and further in old age ($P < 0.001$; Fig. 3B); the content of collagen type IIIα1 chain was increased by about twofold in both middle-aged and old age compared to young mice ($P < 0.05$; Fig. 3D). Quantitative RT–PCR showed a fourfold increase in mRNA for collagen type Iα2 chain in the renal cortex of old mice ($P < 0.01$) but not in the middle-aged mice (Fig. 3C). In contrast, there was a progressive increment in collagen type IIIα1 chain mRNA through middle age to old age, reaching significance in
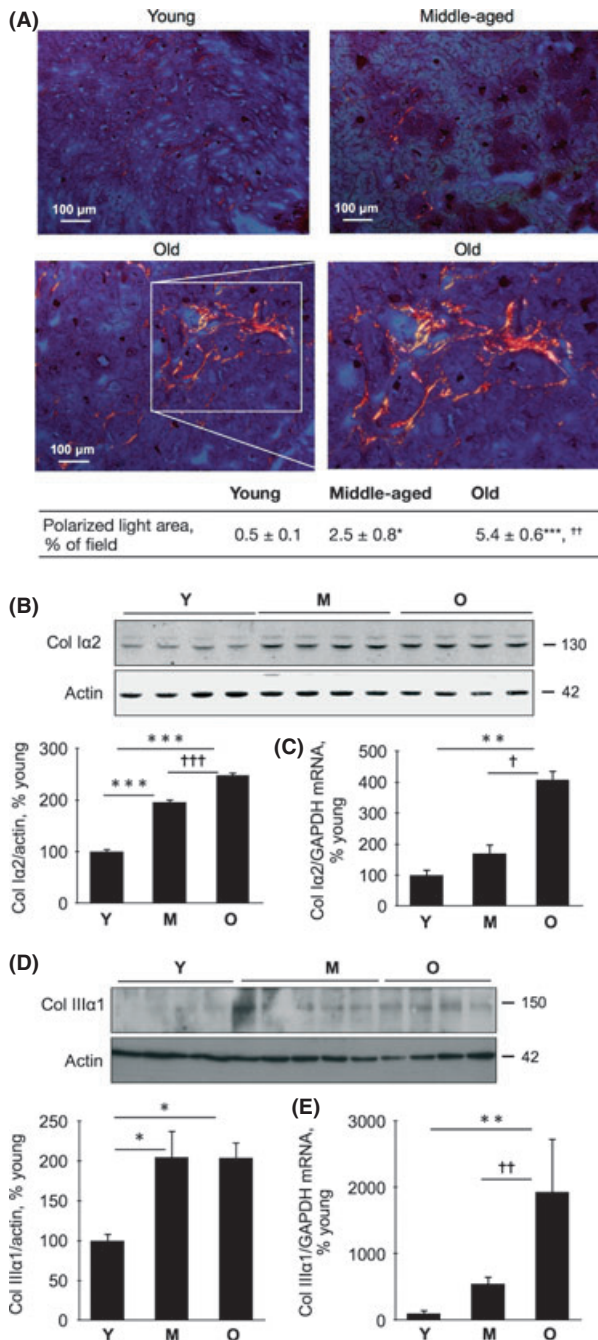
(A)

	Young	Middle-aged	Old
Polarized light area, % of field	0.5 ± 0.1	2.5 ± 0.8*	5.4 ± 0.6***, ††

(B)

(C)

(D)

(E)

Fig. 3 Expression of collagen types I and III in renal parenchyma in young (Y), middle-aged (M), and old (O) mice. (A) Kidney sections were stained with Sirius Red and examined under polarized light to detect cross-linked type I and type III collagens. The boxed area in the bottom left panel is enlarged in the bottom right panel to show anatomical details of the stained area. Composite mean ± SE data from 3 to 4 mice in each group are shown in a table (*$P < 0.05$, ***$P < 0.001$ vs. young mice; ††<0.01 vs. middle-aged mice by ANOVA). (B, D) Equal amounts of renal cortical homogenates from mice were separated by SDS-PAGE and immunoblotted with a specific antibody against either collagen type Iα2 chain or collagen type IIIα1 chain. Composite mean ± SE data from 4 to 5 mice in each group are shown in a histogram (*$P < 0.05$, ***$P < 0.001$ vs. young mice; †††<0.001 vs. middle-aged mice by ANOVA). (C) Quantitative RT–PCR was performed to assess changes in mRNA for collagen types Iα2 chain; **$P < 0.01$ vs. young mice, †$P < 0.05$ vs. middle-aged mice ($n = 10$ mice in each group). (E) Quantitative RT–PCR for type IIIα1 chain mRNA (**$P < 0.01$ vs. young, ††$P < 0.01$ vs. middle-aged mice by ANOVA, $n = 5$–9 mice in each group).

the latter phase ($P < 0.01$; Fig. 3E). These data suggested a transcriptional mechanism for increase in collagen type III in renal aging, in agreement with a recent report (Abrass et al., 2011).

We also examined the status of matrix fibronectin content in the aging kidney. Expression of fibronectin protein was increased in the kidneys in both middle-aged and old mice ($P < 0.01$; Fig. S1A, Supporting information); this was associated with unchanged mRNA content (Fig. S1B), suggesting nontranscriptional mechanisms. These data suggest that distinct regulatory mechanisms contribute to increase in individual matrix proteins in the aging kidney.

Differences in correlation between collagen type Iα2 chain mRNA and protein in the middle-aged and old mice suggested distinct mechanisms for its accumulation in the two phases of aging, that is, nontranscriptional mechanism(s) in the middle age and transcriptional mechanism in old age. Zinc finger enhancer–binding transcription factors, ZEB1 and ZEB2, regulate collagen synthesis and are under the control of TGFβ (Brabletz & Brabletz, 2010). ZEB1 binds to an E box in the promoter of collagen type Iα2 and inhibits its transcription (Kato et al., 2007). The expression of renal ZEB1 was increased in the old mice ($P < 0.05$) but not in the middle-aged mice (Fig. 4A). ZEB2 content in the kidney was increased at middle age ($P < 0.01$) and significantly decreased in old mice ($P < 0.05$ vs. young and $P < 0.001$ vs. middle-aged mice; Fig. 4B).
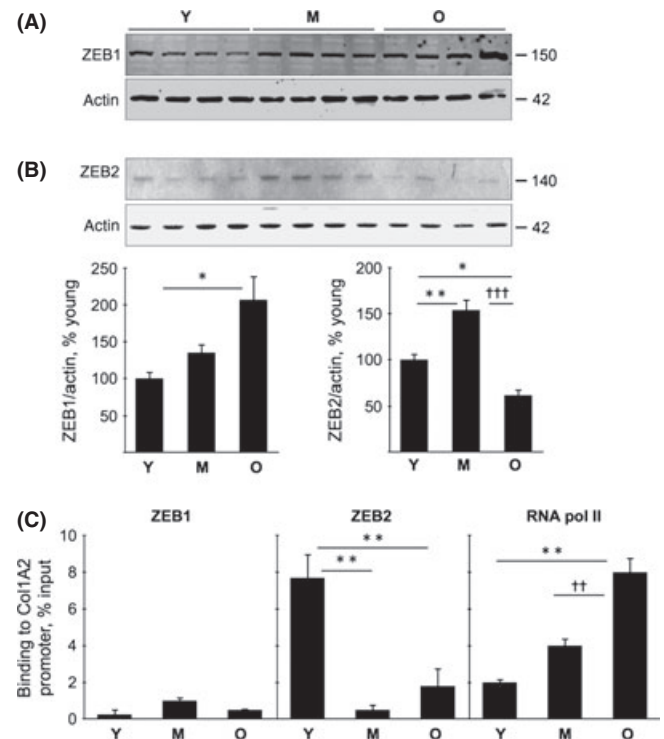
(A)

(B)

(C)

Fig. 4 ZEB1 and ZEB2 contents and their binding to the collagen Iα2 promoter in young (Y), middle-aged (M), and old (O) mice. Immunoblotting of equal amounts of renal cortical homogenates was performed to assess changes in the expression of ZEB1 (A) and ZEB2 (B) (*$P < 0.05$, **$P < 0.01$ vs. young, †††$P < 0.001$ vs. middle-aged mice by ANOVA, $n = 6$ mice in each group). Histograms of composite data for each protein are shown in the lower panels. (C) Chromatin immunoprecipitation (ChIP) assay was performed for the binding of ZEB1, ZEB2, and RNA polymerase II (RNA Pol II) to the collagen type Iα2 promoter as described in Methods. There was no significant change in ZEB1 binding to the promoter. ZEB2 binding to the promoter was decreased in the middle-aged and old mice (**$P < 0.01$ vs. young by ANOVA, $n = 4$–6 mice in each group). RNA Pol II binding to the promoter was increased progressively with aging (**$P < 0.01$ vs. young, ††$P < 0.01$ vs. middle-aged mice by ANOVA, $n = 4$–6 mice in each group).

We next performed Chromatin immunoprecipitation (ChIP) analysis to explore whether changes in ZEB1 and ZEB2 content were associated with corresponding differences in their binding to the collagen type Iα2 promoter. Despite increase in its expression, binding of ZEB1 to the collagen type Iα2 promoter in the renal cortex was unchanged in the old mice compared to young mice (Fig. 4C); it was unchanged in middle-aged mice. Although ZEB2 expression was increased at middle age, its binding to promoter was significantly decreased ($P < 0.01$ vs. young mice; Fig. 4C); in old mice, ZEB2 expression was decreased, which was associated with reduction in its binding to the collagen type Iα2 promoter ($P < 0.01$). In contrast, the binding of RNA polymerase II to the promoter was increased in middle-aged and old mice, reaching significance in the latter ($P < 0.01$; Fig. 4C). These data suggest the following: (i) In the kidney of old mice, reduction in ZEB1 binding to the promoter is not required for augmenting the transcription of collagen type Iα2 mRNA; however, reduction in ZEB2 binding to the promoter could facilitate its transcription. (ii) Because mRNA for collagen type Iα2 did not increase in the middle-aged mice (Fig. 3C), increase in binding of RNA polymerase II and reduction in ZEB2 binding to the promoter are not sufficient to promote its transcription. There must be other regulators that inhibit transcription or accelerate mRNA decay of collagen type Iα2 chain in the kidneys of middle-aged mice.

While the increment in collagen type Iα2 protein in the kidney in old mice was likely due to augmented transcription, in the middle-aged mice, it was not associated with the increase in mRNA content (Fig. 3B, C), suggesting nontranscriptional mechanisms such as augmented efficiency of mRNA translation and/or decreased degradation. We performed a polysome assay to test the former possibility. An mRNA that is targeted for translation is bound by several 80S ribosomal units forming the polysome (Feliers *et al.*, 2005; Kasinath *et al.*, 2009). Polysomes are selectively distributed to the denser fractions on a sucrose gradient. Assay for collagen type Iα2 chain mRNA showed that whereas approximately 20% of the mRNA was present in the denser fractions that contain polysomes in the young mice, it was reduced to approximately 10% in the middle-aged mice (Fig. 5A vs. B). These data show that there was no evidence of increased efficiency of translation of collagen type Iα2 mRNA in the kidneys of middle-aged mice. Because mRNA was not changed and polysome analysis did not support augmented translation, it is likely that decreased degradation accounts for the accumulation of collagen type Iα2 in the kidney in the middle age. The distribution of collagen type Iα2 mRNA into polysomal fractions was increased in the old mice compared to young mice (approximately 45% vs. 20%; Fig. 5A vs. C). This is predictable because increase in mRNA content of collagen type Iα2 seen in the kidneys in the old mice (Fig. 3C) would drive translation, resulting in increase in its protein expression (Fig. 3B); these data do not preclude a contributory role for decreased degradation in collagen accumulation in old mice. Taken together, our data suggest that age-phase-specific regulation exists for the accumulation of collagen type I α2 chain in the kidney in aging.

Activation of TGFβ and SMAD3 in the aging kidney

TGFβ activation contributes importantly to renal fibrosis in a variety of diseases including diabetic nephropathy and obstructive uropathy (Kato *et al.*, 2007; Chung *et al.*, 2010). Because progressive accumulation of extracellular matrix proteins is a prominent feature of aging in mice, we investigated the regulation of TGFβ expression and whether its signaling pathway was activated. Immunoblotting showed increment in TGFβ protein in the kidney during aging, reaching significance in old mice ($P < 0.05$; Fig. 6A). TGFβ mRNA content in the kidney showed a more
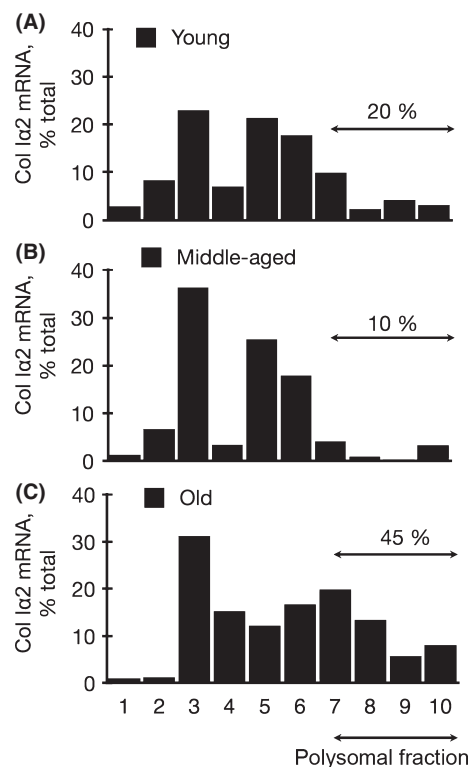

Fig. 5 Polysomal assay in young (Y), middle-aged (M), and old (O) mice. Postnuclear preparations from the renal cortex of mice were separated into ten fractions on a 15–40% sucrose gradient, and mRNA for collagen type Iα2 was detected by RT–PCR. The percentage of total mRNA for collagen type Iα2 distributed to fractions 7–10 represents that bound to 80S ribosome and ready for translation; note the increment in this fraction of mRNA in the old mice. Mean data from two mice from each group are shown.

than threefold increment in the old mice ($P < 0.01$ vs. young and $P < 0.05$ vs. middle-aged mice; Fig. 6B), in agreement with previous reports (Zheng *et al.*, 2003; Wiggins *et al.*, 2010). Ligand-activated TGFβ receptor complex phosphorylates SMAD3 on Ser423/425, which translocates to the nucleus in association with Smad4 and binds to the promoters of matrix genes and augments their transcription (Sanchez & Sharma, 2009). Immunoblotting showed increase in phosphorylated SMAD3 in the renal cortex from middle-aged and old mice ($P < 0.01$, Fig. 6C). Chromatin immunoprecipitation analysis showed a nearly threefold increase in the binding of SMAD3 to the collagen type Iα2 promoter in the kidneys of old mice but not in the kidneys of middle-aged mice (Fig. S2, Supporting information). These data show that renal aging is associated with the activation of the canonical TGFβ signaling pathway that is evident in the middle age and persists into old age; Smad3 appears to participate in augmenting the transcription of collagen type I α2 in the kidneys of old mice.

Recent studies have implicated miRs in pro-fibrotic actions of TGFβ. TGFβ-SMAD3 signaling system augments the production of miR-21 by facilitating its maturation (Davis *et al.*, 2008); renal fibrosis in ureteral obstruction and ischemia–reperfusion injury is dependent on miR-21 (Chau *et al.*, 2012). The renal cortical content of miR-21 was increased in the old mice compared to both young mice ($P < 0.001$) and middle-aged mice ($P < 0.01$; Fig. 6D). One of the targets of miR-21 is Sprouty, of which four homologs exist in mammals. Sprouty-1 is an inhibitor of growth factor signaling (Cabrita & Christofori, 2008). Sprouty expression is reduced in cardiac fibrosis associated with miR-21 increment (Thum
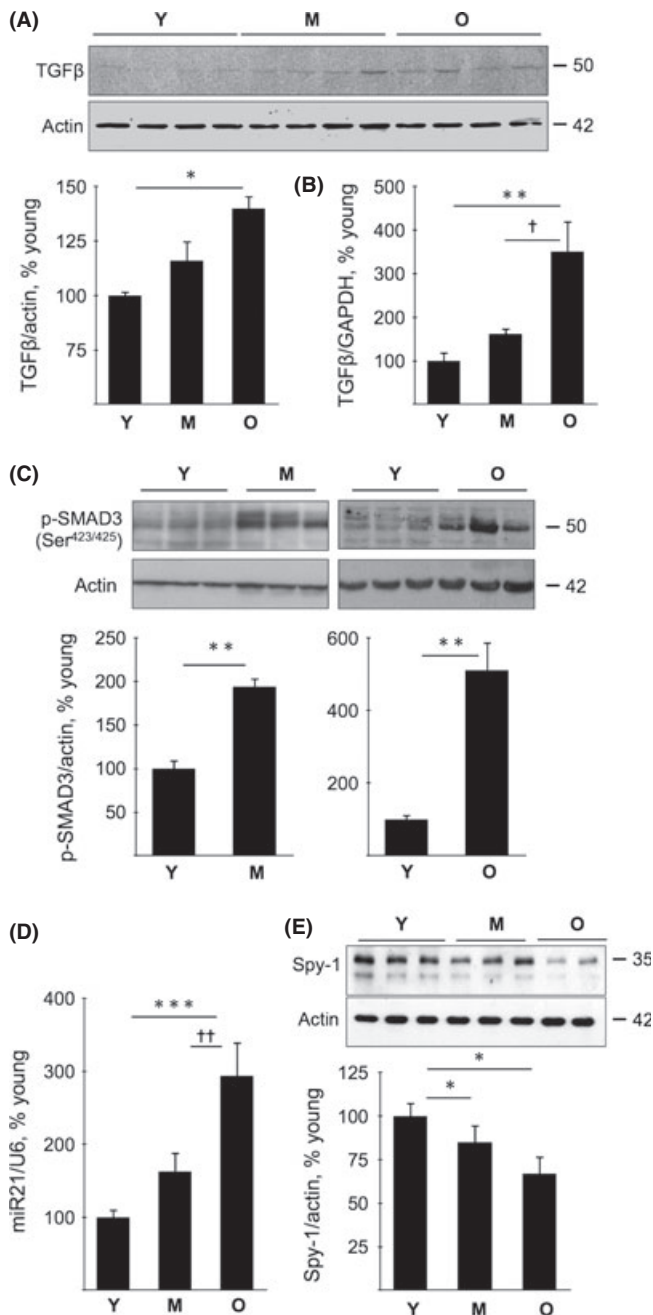
Fig. 6 TGFβ expression and activation, miR21 and Sprouty expression in young (Y), middle-aged (M), and old (O) mice. (A) Immunoblotting of renal cortical homogenates was performed to assess changes in the expression of TGFβ in the middle-aged and old mice. Composite mean ± SE data from four mice in each group are shown in a histogram (*$P < 0.05$ vs. young mice by ANOVA). (B) Quantitative RT–PCR was performed to assess TGFβ mRNA. Composite mean ± SE data from 5 to 6 mice in each group are shown in a histogram (**$P < 0.01$ vs. young mice; †$P < 0.05$ vs. middle-aged mice by ANOVA). (C) Immunoblot analysis of Smad3 phosphorylation in kidney cortical homogenates (representative data from 3 to 6 mice in each group, **$P < 0.01$ vs. young mice). (D) Real-time PCR was performed to assess changes in miR-21 and U6, the latter serving as control. Composite mean ± SE data from 7 to 8 mice in each group are shown in a histogram (***$P < 0.001$ vs. young mice, ††$P < 0.01$ vs. middle-aged mice by ANOVA). (E) Immunoblot analysis of Sprouty-1 (Spy-1) expression in kidney cortical lysates. Composite mean ± SE data from 6 to 8 mice in each group are shown in a histogram (*$P < 0.05$ vs. young mice by ANOVA).

et al., 2008) and in diabetic nephropathy by the activation of miR-29c (Long *et al.*, 2011). A reduction in renal cortical expression of Sprouty-1 ($P < 0.05$) was observed during aging (Fig. 6E). Not all miR-21 targets were affected in the aging kidney. Phosphatase and tensin homolog deleted in chromosome 10 (PTEN) is a phosphatase that inhibits signaling of phosphatidylinositol (PI) 3 kinase by dephosphorylating PI 3-4-5 trisphosphate; PTEN translation is inhibited by high glucose-induced miR-21 in renal mesangial cells (Dey *et al.*, 2011). The expression of PTEN was unchanged in the renal cortex of middle-aged mice and old mice (Fig. S3A, Supporting information).

There was selectivity also in aging-associated changes in kidney miRs that are under regulation by TGFβ. Thus, there was no change in the expression of miR-192, miR-200a, and miR-200b (Fig. S3B–D). miR-192 has been implicated in renal matrix protein accumulation in diabetes (Kato *et al.*, 2007). The renal cortical content of miR-200c was increased in the old mice compared to young or middle-aged mice ($P < 0.01$; Fig. S3E). ZEB2 is one of the targets of miR-200c; there are several consensus sites for miR-200c binding in the 3′untranslated region of ZEB2, and miR-200c inhibits ZEB2 translation (Park *et al.*, 2008). Corresponding to the increment in miR-200c in the kidneys of old mice, the expression of ZEB2 protein was decreased (Fig. 4B), suggesting a functional role for miR-200c. Conversely, reduction in ZEB2 can lead to increased expression of miR-200c; a mutually inhibitory regulation between miR-200 family and ZEBs has been described (Brabletz & Brabletz, 2010). There was a trend toward decreased expression of miR-200c in the kidneys from middle-aged mice (Fig. S3E); it coincided with increase in ZEB2 expression (Fig. 4B). These data suggest that miR-200c could regulate ZEB2 expression in the kidney during aging.

Discussion

Our data show that aging-induced increase in renal matrix protein content, albuminuria, and elevation in cystatin C are associated with the activation of TGFβ/SMAD3 canonical signaling pathway and increase in the expression of select miRs. The regulatory mechanisms contributing to accumulation of extracellular matrix in the aging kidney vary depending on the protein and the phase of aging process. Aging changes in the kidney evaluated in this study, that is, TGFβ activation, miR increment and matrix accumulation, albuminuria, and reduction in clearance function, are evident in the middle age suggesting senescent changes in the kidney have an early onset and a progressive course.

TGFβ promotes both glomerular and tubulointerstitial fibrosis, which contribute to the loss of renal function (Liu, 2011). TGFβ binding to type II receptor promotes the latter to dimerize with the type I receptor (activin-like kinase 5). In the TGFβ1 canonical pathway, the activated TGFβ1 receptor complex catalyzes Ser phosphorylation of receptor SMAD3. Phosphorylated SMAD3 binds to SMAD4 and is translocated to the nucleus, where, along with other transcription factors, it promotes transcription of genes encoding matrix proteins; SMAD3 activity is inhibited by SMAD7 (Chen *et al.*, 2010). Interestingly, SMAD2, another SMAD that binds TGFβ receptor, appears to have an inhibitory effect on TGFβ-induced renal matrix synthesis (Meng *et al.*, 2010). Chromatin immunoprecipitation analysis showed that SMAD3 binding to the collagen type Iα2 promoter was increased at old age suggesting a role in collagen transcription in aging of the kidney. However, in the kidneys of middle-aged mice, neither the SMAD3 binding to the collagen type Iα2 promoter nor mRNA content of the collagen was increased, suggesting nontranscriptional mechanisms, that is, augmented efficiency of mRNA translation and/or decreased degradation. TGFβ activates mRNA translation to increase the synthesis of proteins including matrix

proteins in kidney mesangial cells (Ghosh Choudhury & Abboud, 2004). Because polysomal assay did not suggest augmented translation, it is likely that decreased degradation contributes to accumulation of collagen type Iα2 chain in the kidney in middle-aged mice; future studies will explore this possibility. TGFβ may affect matrix content by regulating the activity of factors that govern matrix degradation. Thus, our data show that increment in collagen type Iα2 chain content in middle age and old age involves distinct mechanisms. In the case of collagen type III, our data suggest transcription as the main mechanism in the aging kidney. Recent investigations indicate that alteration in epigenetic factors exerts control over transcription of collagen type III in the kidney in the aging rat (Abrass *et al.*, 2011). Adenovirus-mediated overexpression of TGFβ in kidney glomeruli is associated with augmented protein losses in the urine (Ghayur *et al.*, 2012), suggesting in the aging mouse, TGFβ may contribute to albuminuria.

The mechanisms by which TGFβ regulates cellular events including renal fibrosis include miRs. Of the several miRs stimulated by TGFβ, we found consistent increase in the content of miR-21 during renal aging. TGFβ can augment miR-21 content by promoting maturation of its precursor (Davis *et al.*, 2008). Recent studies have assigned an important role for miR-21 in pulmonary fibrosis (Liu *et al.*, 2010) although its contribution to cardiac fibrosis has been contested (Thum *et al.*, 2008; Patrick *et al.*, 2010). Increased miR-21 has been implicated in renal fibrosis associated with ischemia–reperfusion injury, anti-Thy1 glomerulonephritis, ureteral obstruction, and diabetes (Denby *et al.*, 2011; Dey *et al.*, 2011; Chau *et al.*, 2012).

The mechanism by which miR-21 elicits a fibrotic response can vary with the model of renal disease. In ischemia–reperfusion injury and obstruction, pro-fibrotic actions of miR-21 are mediated by changes in PPARα (Chau *et al.*, 2012). In diabetes, miR-21 reduces PTEN expression in the kidney to stimulate PI3 kinase signaling pathway, leading to augmented synthesis of matrix proteins (Dey *et al.*, 2011). Because PTEN expression was unaffected in the aging kidney, other pathways are probably recruited by miR-21 to promote renal fibrosis. In this context, we examined the status of Sprouty-1, a target of miR-21 and an inhibitor of signaling by growth factors. Long *et al.* (2011) have shown that renal matrix accumulation in diabetes is associated with reduced Sprouty expression by suppression of its translation by miR-29c; restoration of Sprouty by antisense oligo against miR-29c reduced matrix fibronectin in diabetic mice, perhaps, by inhibition of Rho kinase. The molecular mechanism by which Sprouty may affect changes in the aging kidney needs to be investigated. Changes in miRs can vary between models of renal fibrosis. For instance, miR-192 is increased in the kidney in diabetes (Kato *et al.*, 2007); we did not find a significant change in miR-192 expression in the aging kidney. The aforementioned studies suggest that renal fibrosis has unique mechanisms, including involvement of miRs and their targets, which vary with the context (Kasinath & Feliers, 2011). Although miRs are but one of the many factors that affect gene expression, individual miRs can influence the outcome in a context-specific manner. For instance, neutralization of miR-29c or miR-21 ameliorated renal matrix abnormalities in diabetes, ureteral obstruction, and ischemia (Long *et al.*, 2011; Chau *et al.*, 2012). A schematic diagram of pathways potentially underlying kidney manifestations seen in old mice is shown in Fig. 7.

Renal fibrosis represents a failed wound healing process, which commonly involves TGFβ (Liu, 2011). Factors that induce TGFβ expression in the aging kidney are not well understood. Angiotensin II, oxidative stress, and advanced glycation end products are capable of inducing TGFβ in the aging kidney (Choudhury & Levi, 2011). Augmenting PPARγ activity with pioglitazone inhibits TGFβ signaling in
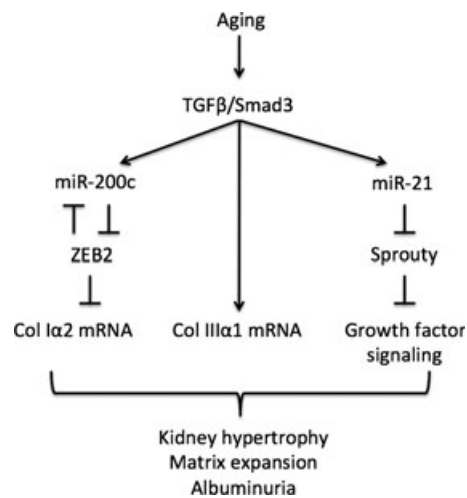

Fig. 7 A schematic diagram shows pathways involved in changes in the kidney in old mice reported in this study.

the kidney in the aging rat, assigning a regulatory role for the nuclear receptor possibly through inhibition of mitochondrial oxidative stress (Yang *et al.*, 2009). There are several limitations to our study. We took a candidate approach to explore miR regulation based on regulation by TGFβ and involvement in renal fibrosis; an unbiased microarray is likely to reveal dysregulation of many other miRs. Our data do not provide a cause and effect link between molecular events described and structural and functional changes in renal senescence. However, our data suggest several potential sites for the investigation of mechanisms underlying aging-related changes in the kidney and intervention, that is, TGFβ, miR-21, Sprouty-1. Because our data show that molecular events and the downstream phenotypes of renal aging are in place in the middle age, interventions will need to be initiated early, and it is likely that a multi-pronged approach will be needed. A more complete understanding of molecular events may reveal additional targets for intervention and improvement of health span.

Experimental procedures

Animals

We employed female C57BL6 mice (National Institute of Aging). Studies were performed on young mice (4–6 months of age), middle-aged (18 months of age), and old mice (26–32 months of age) because it is important to track aging-related changes in an age-linear fashion in order to distinguish them from changes related to the end of life pathologies (Miller & Nadon, 2000). The mice had free access to standard chow and water and maintained on a 12-h light/dark cycle. Before sacrifice, individual mice were placed in metabolic cages for 24-h urine collection. Commercial kits were used to measure albumin (Bethyl Laboratories, Montgomery, TX, USA), creatinine (Enzo Life Sciences Inc, Farmingdale, NY, USA), and serum cystatin C (Quantikine ELISA assay; R&D Systems, Minneapolis, MN, USA). Blood glucose concentration was measured by a glucometer (Ascensia Elite XL, Mishawaka, IN, USA). At the time of sacrifice, both kidneys were removed and weighed. A part of the kidney section was paraffin-embedded or snap-frozen in liquid nitrogen for image analysis. The Institutional Animal Care and Use Committee approved the studies.

Morphometric analysis

Glomerular morphometry was performed as described in the study by Sataranatarajan *et al.* (2007). Photographic images were taken from 25 random glomeruli from each mouse using an Olympus AX70 research microscope equipped with a 20× objective and DP70 digital camera (Olympus America Inc, Melville, NY, USA). In each digital image, the circumference of the glomerular tuft was outlined using the polygonal tracing tool and area calculated using Image-Pro Plus 4.5 software (Media Cybernetics, Silver Spring, MD, USA). All images were calibrated to a stage micrometer. Mesangial matrix in PAS stained formalin-fixed tissue was also measured by digital analysis using the segmentation tool of Image-Pro Plus and quantified as a percentage of the total glomerular tuft area. In addition, cross-linked collagens were detected by Sirius Red–stained frozen sections under polarized light. Refracted light representing collagen types I and III staining was segmented and quantified as a percentage of the total field area.

Immunoblot analysis

Immunoblot analysis was performed as described (Sataranatarajan *et al.*, 2007; Mariappan *et al.*, 2011; Lee *et al.*, 2012). Equal amounts of renal cortical protein from homogenates were resolved by SDS-PAGE and transferred to a nitrocellulose membrane. The membrane was probed with the primary antibody overnight at 4 °C. The following antibodies were employed: fibronectin and actin (Sigma, St. Louis, MO, USA), collagen type Iα2 chain (Proteintech Group Inc, Chicago, IL, USA), ZEB1 (Bethyl Laboratories), collagen type IIIα1 chain, Sprouty-1, PTEN and ZEB2 (Santa Cruz Biotechnology, Santa Cruz, CA, USA), TGFβ, RNA polymerase II (Abcam, Cambridge, MA, USA), phospho-SMAD3 (Origene, Rockville, MD, USA), and SMAD3 (Zymed, San Francisco, CA, USA). Membranes were extensively washed and incubated with secondary antibodies linked to horseradish peroxidase (Jackson ImmunoResearch Laboratories, West Grove, PA, USA) or IRDye (Rockland Immunochemicals, Gilbertsville, PA, USA). Proteins were visualized using enhanced chemiluminescence reagent. Alternatively, Odyssey infrared imaging system (Li-Cor Biosciences, Lincoln, NE, USA) was used to detect fluorochrome-coupled antibody. Signal intensities were quantified using the Scion image software (Scion Corporation, Frederick, MD, USA).

Real-time PCR

Total RNA was isolated using the TRIzol reagent (Invitrogen, Carlsbad, CA, USA). RNA yield and purity were determined by measuring the absorbance at 260 and 280 nm. First-strand cDNA was synthesized from 1 µg of total RNA using Reaction Ready First-strand cDNA synthesis kit (SABiosciences, Valencia, CA, USA). Fifty nanogram of cDNA samples was PCR amplified using primers for TGFβ, collagen type Iα2 chain, collagen type IIIα1 chain, fibronectin or GAPDH and SYBR green master mix (SABiosciences). Real-time PCR was performed using a Realplex Mastercycler instrument. Relative mRNA expression was calculated using the $\Delta\Delta^{C_t}$ method (Sataranatarajan *et al.*, 2007; Mariappan *et al.*, 2008, 2011).

TaqMan miR assay for mature miR expression analysis

Total RNA was isolated as described above. Primers specific for mature miRs and U6 were used for miR quantification. Briefly, cDNA was prepared using the RT miR-specific stem loop primer from TaqMan microRNA reverse transcription kit (Applied Biosystems, Carlsbad, CA, USA). cDNA was used to perform the real-time PCR using the miR-specific TaqMan primers (Applied Biosystems). The assay was performed in triplicate. The fold change was determined between U6 control and mature miRs.

Chromatin immunoprecipitation assay

Chromatin immunoprecipitation was performed as described in the study by Nelson *et al.* (2009). Cross-linked chromatin from the kidney cortex was sheared by sonication and used for immunoprecipitation using ChIP-validated antibodies. DNA was purified from the immunoprecipitates using a 10% Chelex (Bio-Rad, Hercules, CA, USA) solution supplemented with proteinase K (0.2 mg mL^{-1} final), incubated at 55 °C for 30 min followed by boiling for 15 min, and used for quantitative PCR using primers spanning E box region (Kato *et al.*, 2007) to detect binding of ZEB proteins and primers spanning the +1 to −1000 bases of the collagen type Iα2 promoter for RNA pol II binding.

Polysome assay

The protocol has been previously described (Feliers *et al.*, 2005). Slices of kidney cortex were homogenized in 0.4 mL of buffer containing 10 mM Tris (pH 7.5), 250 mM KCl, and 2 mM MgCl$_2$. A 10% Tween-80, 5% (w/v) deoxycholate mix was added to the lysates, which were centrifuged at 4 °C for 10 min at 20 800 *g*. The postnuclear supernatants were laid on top of 15–40% sucrose gradient and centrifuged for 90 min at 200 000 *g*. After ultracentrifugation, the gradients were separated into ten fractions, and RNA was extracted from each fraction using TRIzol (Invitrogen). Reverse transcription of mRNAs was performed using iScript cDNA Synthesis Kit (Bio-Rad). The resulting cDNAs were used for quantitative PCR (qPCR) using primers in a RT^2 qPCR Master Mix (SABiosciences/Qiagen) and a MasterCycler RealPlex4 (Eppendorf, Hauppauge, NY, USA).

Statistical analysis

Data were expressed as mean ± SE. Comparisons among the three age groups were performed by analysis of variance (ANOVA) with post-testing correction by the Newman–Keuls method employing the GraphPad Prism 4 software (GraphPad Software, Inc., La Jolla, CA, USA); analyses between two groups were performed by the Student's *t*-test. Data were considered statistically significant at $P < 0.05$.

Acknowledgments

Author contributions

K.S., D.F., M.M.M., H.J.L., M.J.L., R.T.D., and H.Y. performed experiments and assisted in data analysis; J.L.B., G.G.C., H.V.R., A.R. took part in data analysis; K.S., D.F., and B.S.K. wrote the manuscript; B.S.K. designed the study.

References

Abrass CK, Adcox MJ, Raugi GJ (1995) Aging-associated changes in renal extracellular matrix. *Am. J. Pathol.* **146**, 742–752.

Abrass CK, Hansen K, Popov V, Denisenko O (2011) Alterations in chromatin are associated with increases in collagen III expression in aging nephropathy. *Am. J. Physiol. Renal. Physiol.* **300**, F531–F539.

Brabletz S, Brabletz T (2010) The ZEB/miR-200 feedback loop–a motor of cellular plasticity in development and cancer? *EMBO Rep.* **11**, 670–677.

Cabrita MA, Christofori G (2008) Sprouty proteins, masterminds of receptor tyrosine kinase signaling. *Angiogenesis* **11**, 53–62.

Chau BN, Xin C, Hartner J, Ren S, Castano AP, Linn G, Li J, Tran PT, Kaimal V, Huang X, Chang AN, Li S, Kalra A, Grafals M, Portilla D, MacKenna DA, Orkin SH, Duffield JS (2012) MicroRNA-21 promotes fibrosis of the kidney by silencing metabolic pathways. *Sci. Transl. Med.* **4**, 21ra118.

Chen HY, Huang XR, Wang W, Li JH, Heuchel RL, Chung AC, Lan HY (2010) The protective role of Smad7 in diabetic kidney disease: mechanism and therapeutic potential. *Diabetes* **60**, 590–601.

Choudhury D, Levi M (2011) Kidney aging–inevitable or preventable? *Nat. Rev. Nephrol.* **7**, 706–717.

Chung AC, Huang XR, Meng X, Lan HY (2010) miR-192 mediates TGF-beta/Smad3-driven renal fibrosis. *J. Am. Soc. Nephrol.* **21**, 1317–1325.

Davis BN, Hilyard AC, Lagna G, Hata A (2008) SMAD proteins control DROSHA-mediated microRNA maturation. *Nature* **454**, 56–61.

Denby L, Ramdas V, McBride MW, Wang J, Robinson H, McClure J, Crawford W, Lu R, Hillyard DZ, Khanin R, Agami R, Dominiczak AF, Sharpe CC, Baker AH (2011) miR-21 and miR-214 are consistently modulated during renal injury in rodent models. *Am. J. Pathol.* **179**, 661–672.

Dey N, Das F, Mariappan MM, Mandal CC, Ghosh-Choudhury N, Kasinath BS, Choudhury GG (2011) MicroRNA-21 orchestrates high glucose-induced signals to TOR complex 1, resulting in renal cell pathology in diabetes. *J. Biol. Chem.* **286**, 25586–25603.

Feliers D, Duraisamy S, Barnes JL, Ghosh-Choudhury G, Kasinath BS (2005) Translational regulation of vascular endothelial growth factor expression in renal epithelial cells by angiotensin II. *Am. J. Physiol. Renal. Physiol.* **288**, F521–F529.

Ghayur A, Liu L, Kolb M, Chawla A, Lambe S, Kapoor A, Margetts PJ (2012) Adenovirus-mediated gene transfer of TGF-beta1 to the renal glomeruli leads to proteinuria. *Am. J. Pathol.* **180**, 940–951.

Ghosh Choudhury G, Abboud HE (2004) Tyrosine phosphorylation-dependent PI 3 kinase/Akt signal transduction regulates TGFbeta-induced fibronectin expression in mesangial cells. *Cell. Signal.* **16**, 31–41.

Glassock RJ, Rule AD (2012) The implications of anatomical and functional changes of the aging kidney: with an emphasis on the glomeruli. *Kidney Int.*, **82**, 270–277.

Grimm PC, Nickerson P, Gough J, McKenna R, Stern E, Jeffery J, Rush DN (2003) Computerized image analysis of Sirius Red-stained renal allograft biopsies as a surrogate marker to predict long-term allograft function. *J. Am. Soc. Nephrol.* **14**, 1662–1668.

Ho J, Ng KH, Rosen S, Dostal A, Gregory RI, Kreidberg JA (2008) Podocyte-specific loss of functional microRNAs leads to rapid glomerular and tubular injury. *J. Am. Soc. Nephrol.* **19**, 2069–2075.

Ka SM, Yeh YC, Huang XR, Chao TK, Hung YJ, Yu CP, Lin TJ, Wu CC, Lan HY, Chen A (2012) Kidney-targeting Smad7 gene transfer inhibits renal TGF-beta/MAD homologue (SMAD) and nuclear factor kappaB (NF-kappaB) signalling pathways, and improves diabetic nephropathy in mice. *Diabetologia* **55**, 509–519.

Kasinath BS, Feliers D (2011) The complex world of kidney microRNAs. *Kidney Int.* **80**, 334–337.

Kasinath BS, Feliers D, Sataranatarajan K, Ghosh Choudhury G, Lee MJ, Mariappan MM (2009) Regulation of mRNA translation in renal physiology and disease. *Am. J. Physiol. Renal. Physiol.* **297**, F1153–F1165.

Kato M, Zhang J, Wang M, Lanting L, Yuan H, Rossi JJ, Natarajan R (2007) MicroRNA-192 in diabetic kidney glomeruli and its function in TGF-beta-induced collagen expression via inhibition of E-box repressors. *Proc. Natl Acad. Sci. USA* **104**, 3432–3437.

Kume S, Uzu T, Horiike K, Chin-Kanasaki M, Isshiki K, Araki S, Sugimoto T, Haneda M, Kashiwagi A, Koya D (2010) Calorie restriction enhances cell adaptation to hypoxia through Sirt1-dependent mitochondrial autophagy in mouse aged kidney. *J. Clin. Invest.* **120**, 1043–1055.

Lee HJ, Mariappan MM, Feliers D, Cavaglieri RC, Sataranatarajan K, Abboud HE, Choudhury GG, Kasinath BS (2012) Hydrogen sulfide inhibits high glucose-induced matrix protein synthesis by activating AMP-activated protein kinase in renal epithelial cells. *J. Biol. Chem.* **287**, 4451–4461.

Lindeman RD, Tobin J, Shock NW (1985) Longitudinal studies on the rate of decline in renal function with age. *J. Am. Geriatr. Soc.* **33**, 278–285.

Liu Y (2011) Cellular and molecular mechanisms of renal fibrosis. *Nat. Rev. Nephrol.* **7**, 684–696.

Liu G, Friggeri A, Yang Y, Milosevic J, Ding Q, Thannickal VJ, Kaminski N, Abraham E (2010) miR-21 mediates fibrogenic activation of pulmonary fibroblasts and lung fibrosis. *J. Exp. Med.* **207**, 1589–1597.

Long J, Wang Y, Wang W, Chang BH, Danesh FR (2011) MicroRNA-29c is a signature microRNA under high glucose conditions that targets Sprouty homolog 1, and its in vivo knockdown prevents progression of diabetic nephropathy. *J. Biol. Chem.* **286**, 11837–11848.

Mariappan MM, Shetty M, Sataranatarajan K, Choudhury GG, Kasinath BS (2008) Glycogen synthase kinase 3beta is a novel regulator of high glucose- and high insulin-induced extracellular matrix protein synthesis in renal proximal tubular epithelial cells. *J. Biol. Chem.* **283**, 30566–30575.

Mariappan MM, D'Silva K, Lee MJ, Sataranatarajan K, Barnes JL, Choudhury GG, Kasinath BS (2011) Ribosomal biogenesis induction by high glucose requires activation of upstream binding factor in kidney glomerular epithelial cells. *Am. J. Physiol. Renal. Physiol.* **300**, F219–F230.

Meng XM, Huang XR, Chung AC, Qin W, Shao X, Igarashi P, Ju W, Bottinger EP, Lan HY (2010) Smad2 protects against TGF-beta/Smad3-mediated renal fibrosis. *J. Am. Soc. Nephrol.* **21**, 1477–1487.

Miller RA, Nadon NL (2000) Principles of animal use for gerontological research. *J. Gerontol. A Biol. Sci. Med. Sci.* **55**, B117–B123.

Nelson J, Denisenko O, Bomsztyk K (2009) The fast chromatin immunoprecipitation method. *Methods Mol. Biol.* **567**, 45–57.

Park SM, Gaur AB, Lengyel E, Peter ME (2008) The miR-200 family determines the epithelial phenotype of cancer cells by targeting the E-cadherin repressors ZEB1 and ZEB2. *Genes Dev.* **22**, 894–907.

Patrick DM, Montgomery RL, Qi X, Obad S, Kauppinen S, Hill JA, van Rooij E, Olson EN (2010) Stress-dependent cardiac remodeling occurs in the absence of microRNA-21 in mice. *J. Clin. Invest.* **120**, 3912–3916.

Reed III JF, Kopyt NP (2011) Prevalence of Albuminuria in the U.S. Adult Population Over the age of 40: results from the National Health and Nutrition Examination Survey (1999–2008). *Internet J. Nephrol.* **6**.

Samarakoon R, Overstreet JM, Higgins SP, Higgins PJ (2012) TGF-beta1 –> SMAD/p53/USF2 –> PAI-1 transcriptional axis in ureteral obstruction-induced renal fibrosis. *Cell Tissue Res.* **347**, 117–128.

Sanchez AP, Sharma K (2009) Transcription factors in the pathogenesis of diabetic nephropathy. *Expert Rev. Mol. Med.* **11**, e13.

Sataranatarajan K, Mariappan MM, Lee MJ, Feliers D, Choudhury GG, Barnes JL, Kasinath BS (2007) Regulation of elongation phase of mRNA translation in diabetic nephropathy: amelioration by rapamycin. *Am. J. Pathol.* **171**, 1733–1742.

Song S, Meyer M, Turk TR, Wilde B, Feldkamp T, Assert R, Wu K, Kribben A, Witzke O (2009) Serum cystatin C in mouse models: a reliable and precise marker for renal function and superior to serum creatinine. *Nephrol. Dial. Transplant.* **24**, 1157–1161.

Thum T, Gross C, Fiedler J, Fischer T, Kissler S, Bussen M, Galuppo P, Just S, Rottbauer W, Frantz S, Castoldi M, Soutschek J, Koteliansky V, Rosenwald A, Basson MA, Licht JD, Pena JT, Rouhanifard SH, Muckenthaler MU, Tuschl T, Martin GR, Bauersachs J, Engelhardt S (2008) MicroRNA-21 contributes to myocardial disease by stimulating MAP kinase signalling in fibroblasts. *Nature* **456**, 980–984.

Wiggins JE, Patel SR, Shedden KA, Goyal M, Wharram BL, Martini S, Kretzler M, Wiggins RC (2010) NFkappaB promotes inflammation, coagulation, and fibrosis in the aging glomerulus. *J. Am. Soc. Nephrol.* **21**, 587–597.

Yang HC, Deleuze S, Zuo Y, Potthoff SA, Ma LJ, Fogo AB (2009) The PPARgamma agonist pioglitazone ameliorates aging-related progressive renal injury. *J. Am. Soc. Nephrol.* **20**, 2380–2388.

Zheng F, Plati AR, Potier M, Schulman Y, Berho M, Banerjee A, Leclercq B, Zisman A, Striker LJ, Striker GE (2003) Resistance to glomerulosclerosis in B6 mice disappears after menopause. *Am. J. Pathol.* **162**, 1339–1348.

Zheng F, Cheng QL, Plati AR, Ye SQ, Berho M, Banerjee A, Potier M, Jaimes EA, Yu H, Guan YF, Hao CM, Striker LJ, Striker GE (2004) The glomerulosclerosis of aging in females: contribution of the proinflammatory mesangial cell phenotype to macrophage infiltration. *Am. J. Pathol.* **165**, 1789–1798.

Zhong X, Chung AC, Chen HY, Meng XM, Lan HY (2011) Smad3-mediated upregulation of miR-21 promotes renal fibrosis. *J. Am. Soc. Nephrol.* **22**, 1668–1681.

Supporting Information

Additional Supporting Information may be found in the online version of this article at the publisher's web-site:

Fig. S1 Fibronectin mRNA and protein in young (Y), middle-aged (M) and old (O) mice.

Fig. S2 Binding of SMAD3 to the collagen1α2 (*COL1A2*) promoter.

Fig. S3 Expression of PTEN and miRs 192, 200a, 200b, 200c in young (Y), middle-aged (M) and old (O) mice.